# The Bonding Nature of Some Simple Sigmatropic Transition States from the Topological Analysis of the Electron Localization Function

**ARTICLE** *in* THE JOURNAL OF PHYSICAL CHEMISTRY A · NOVEMBER 2002

Impact Factor: 2.69 · DOI: 10.1021/jp025958q



**5 AUTHORS**, INCLUDING:

Eduardo Chamorro
Universidad Andrés Bello
**79** PUBLICATIONS **1,690** CITATIONS
SEE PROFILE

Badhin Gomez
Universidad La Salle, Arequipa, Perú
**14** PUBLICATIONS **450** CITATIONS
SEE PROFILE

Renato Contreras
University of Chile
**184** PUBLICATIONS **3,880** CITATIONS
SEE PROFILE

Patricio Fuentealba
University of Chile
**153** PUBLICATIONS **4,369** CITATIONS
SEE PROFILE

# The Bonding Nature of Some Simple Sigmatropic Transition States from the Topological Analysis of the Electron Localization Function

**Eduardo Chamorro,[†,*] Juan C. Santos,[†] Badhin Gómez,[‡] Renato Contreras,[‡] and Patricio Fuentealba[†]**

*Departamento de Física, Facultad de Ciencias, Universidad de Chile, Casilla 653, Santiago, Chile, and Departamento de Química, Facultad de Ciencias, Universidad de Chile, Casilla 653, Santiago, Chile*

*Received: April 16, 2002; In Final Form: July 29, 2002*

It is shown that the topological analysis of the electron localization function (ELF), a measure of the local Pauli repulsion, is a useful tool to describe the bonding nature of transition structures of simple pericyclic processes. In this work, we have revisited the [$1_s$,$3_a$]hydrogen, [$1_a$,$3_s$]methyl, and [$1_a$,$3_s$]fluorine simple sigmatropic rearrangements in the allyl system. Results based on the integrated densities over the ELF basins and their related properties at the B3LYP/6-311++G(d,p) level of theory showed explicitly a delocalized structure for the antarafacial ($C_s$) hydrogen rearrangement, a two radical interaction for the methyl suprafacial ($C_2$) migration, and a pair−ion interaction for the fluorine suprafacial ($C_s$) transfer. Results on these well-studied systems confirm the topological analysis of the ELF as a useful descriptor for the study of bonding structure of pericyclic transition states. In this context, the ELF analysis is shown to be a complementary value to the Woodward−Hoffmann rules, which provide an orbital symmetry basis of understanding.

## Introduction

Characterization of the bonding nature of pericyclic transition states plays a fundamental role in chemistry. Hence, energetic considerations, as first-order responses, have received a great deal of attention. However, an analysis of the electron distribution at the external potential determined by nuclei at the transition structure (TS) is a major concern for selectivity issues related with reactivity of the pericyclic paths. Concerning the energetic aspects of chemical reactivity, accurate calculations of activation energies and rates, substituent effects of rates, and kinetic isotope effects have been the major challenge problems for many years in the description of these reaction mechanisms.[1] The Woodward−Hoffmann analysis, based on the conservation of orbital symmetry,[2−9] is the basis for the understanding and systematization of these chemical processes. Particularly interesting are the unimolecular and one step [1,3] sigmatropic rearrangements because of their relevant applications in organic and inorganic synthetic chemistry. Although there is no definitive experimental evidence for a thermal, concerted [1,3]-hydrogen shift in a hydrocarbon system, this possibility has been already pointed out for related systems such as alkyl-substituted allenes, 1-silapropene, and 1-phosphapropene.[10−14] The benchmark [$1_s$,$3_a$] rearrangement of hydrogen in the allyl system (propene) has been extensively studied from a theoretical viewpoint.[15−24] The interest has been mainly devoted to the elucidation and understanding of structural, dynamical, and thermodynamical aspects of such fundamental pericyclic chemical processes. Results, based on several types of calculations, have been finally interpreted in terms of the simple theoretical principles of the Woodward−Hoffmann rules for the conservation of orbital symmetry. In this context, the allowed [$1_s$,$3_a$] TS has been described in the literature basically in terms of "two weakly interacting radicals".[5,24] The analysis of structure and orbital bonding interactions of the transition state yields finally to the intuitive picture of a delocalized process for the [$1_s$,$3_a$]-hydrogen migration. Similarly, the Woodward−Hoffmann allowed [$1_a$,$3_s$]alkyl[25] and halogen migration processes to be conceived on the basis of a suprafacial stereochemistry with inversion at the migrating center.[5,26] Radical or ionic interactions for these TSs can be expected from a purely first-order orbital interaction model.[2−5]

On the other hand, the topological analysis of the electron localization function (ELF) of Becke and Edgecombe[27,28] provides an elegant and convenient partition of the molecular space into basins of attractors that can be interpreted consistently on the basis of simple ideas of chemical bonding based on the Pauli exclusion principle. This methodology has proven to be a practical tool for the description of the nature of chemical bonding in several stationary systems[29−42] as well as in some simple chemical reaction processes.[43−46] Several interesting issues of chemical reactivity and selectivity have been also addressed with this increasingly useful tool.[47−60] A wide range of useful applications of these tools for the treatment of chemical bonds has been found recently over many different fields of chemistry.[61] Following our previous work on the [$1_a$,$3_s$]fluorine migration process in the 3-fluorpropene system,[62] we have explored the bonding nature of related TSs with the aim of examining further the usefulness of the ELF analysis in the context of local aspects of electron distribution and chemical reactivity of pericyclic reactions. The benchmark reactions corresponding to the [$1_s$,$3_a$]hydrogen, [$1_a$,$3_s$]methyl, and [$1_a$,$3_s$]-fluorine sigmatropic shifts in the allyl system have been used as examples to search for new insights that could be obtained from such a partitioning scheme, which is based directly on the local Pauli repulsion effects.[27,28] Our aim is to explore the ELF analysis as a possible descriptor of the electron rearrange-

* To whom correspondence should be addressed. Current address: Departamento de Química, Facultad de Ecología y Recursos Naturales, Universidad Andrés Bello, República 217, Santiago, Chile. Tel: (56-2)-661-8231. Fax: (56-2)661-5679. E-mail: echamorro@abello.unab.cl.

† Departamento de Física.

‡ Departamento de Química.

10.1021/jp025958q CCC: $22.00 
Published on Web 11/05/2002

ment along pericyclic TSs. It must be noted at this point that the analysis based on the ELF does not depend in principle on the orbitals.[28,63] It will be shown explicitly from the present results that the analysis of properties of the electron density integrated over the ELF basins provides a clear picture of the bonding, which complements the Woodward−Hoffmann analysis for these type of reactions. A highly delocalized bonding structure will appear naturally for the [$1_s$,$3_a$] sigmatropic rearrangement of hydrogen while radical-like and ion-pair like structures are obtained for the [$1_a$,$3_s$]methyl and the [$1_a$,$3_s$]-fluorine transfer, respectively.

## Theory

The local function ELF(**r**) has been defined and interpreted in terms of the excess of local kinetic energy density due to the Pauli repulsion, $T(\rho(\mathbf{r}))$ and the Thomas−Fermi kinetic energy density, $T_h(\rho(\mathbf{r}))$[33,34]

$$\mathrm{ELF}(\mathbf{r}) = \frac{1}{1+\left[\frac{T(\mathbf{r})}{T_h(\mathbf{r})}\right]^2} \tag{1}$$

These quantities, when they are evaluated for a single determinantal wave function built from Hartree−Fock (HF) or Kohn−Sham (KS) orbitals, $\varphi_i(\mathbf{r})$, can be written straightforward as

$$T(\mathbf{r}) = \frac{1}{2}\sum_i |\nabla\varphi_i(\mathbf{r})|^2 - \frac{1}{8}\frac{|\nabla\rho(\mathbf{r})|^2}{\rho(\mathbf{r})} \tag{2}$$

$$T_h(\mathbf{r}) = 2.871\rho(\mathbf{r})^{5/3} \tag{3}$$

$$\rho(\mathbf{r}) = \sum_i |\varphi_i(\mathbf{r})|^2 \tag{4}$$

where atomic units have been used. The key term in the ELF is the function $T(\mathbf{r})$ of eq 2, which represents the excess of kinetic energy density due to the Pauli exclusion principle. The final form of the ELF, eq 1, is conveniently ranged between 0 and 1. The chemical interpretation is that a region of the space where the ELF has a high value represents a region of the space where it is probable to find an electron pair. The gradient field of the ELF function provides us with basins of attractors whose properties can be then interpreted in connection with relevant chemical-bonding characteristics. In this context, these properties have been related with the intuitive concepts of localization and delocalization of the electron density[64] through a standard topological population analysis.

Thus, the average population of a basin, $\tilde{N}_i$, is obtained from the integral of the one electron density $\rho(\mathbf{r})$ over the volume of the basin

$$\tilde{N}_i = \int_{\Omega_i} \rho(\mathbf{r})\, d\mathbf{r} \tag{5}$$

and their population variance, $\sigma^2(\tilde{N}_i)$ (i.e., the quantum uncertainty of the basin population), can be calculated in terms of the diagonal elements of the first-order $\rho(\mathbf{r})$ and second-order $\pi(\mathbf{r}_1,\mathbf{r}_2)$ density matrixes

$$\sigma^2(\tilde{N}_i) = \int_{\Omega_i}\int d\mathbf{r}_1 \int_{\Omega_i}\int d\mathbf{r}_2 \pi(\mathbf{r}_1,\mathbf{r}_2) + \tilde{N}_i - [\tilde{N}_i]^2 \tag{6}$$

Therefore, the covariance analysis might be useful for a careful examination of the electronic delocalization involving a pair of basins. Indeed, the relative fluctuation $\lambda(\tilde{N}_i)$, which has been shown as an efficient tool to study delocalization,[33,64] is defined in terms of the above quantities

$$\lambda(\tilde{N}_i) = \frac{\sigma^2(\tilde{N}_i)}{\tilde{N}_i} \tag{7}$$

## Computational Details

All optimizations have been carried out using the Gaussian98 package of programs[65] within the Berny algorithm at the

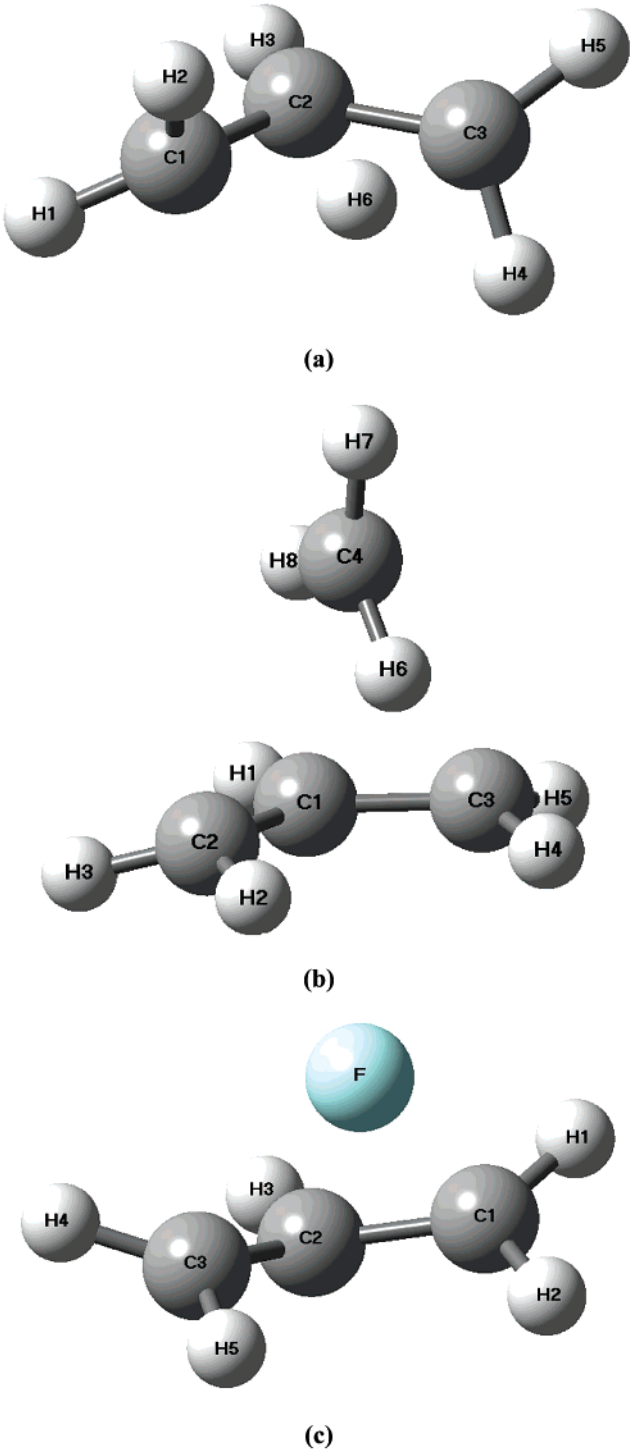


**Figure 1.** Schematic representation of the B3LYP/6-311++G(d,p)-optimized TSs corresponding to the (a) [$1_s$,$3_a$]hydrogen, (b) [$1_a$,$3_s$]-methyl, and (c) [$1_a$,$3_s$]fluorine sigmatropic shift reactions in the allyl system.

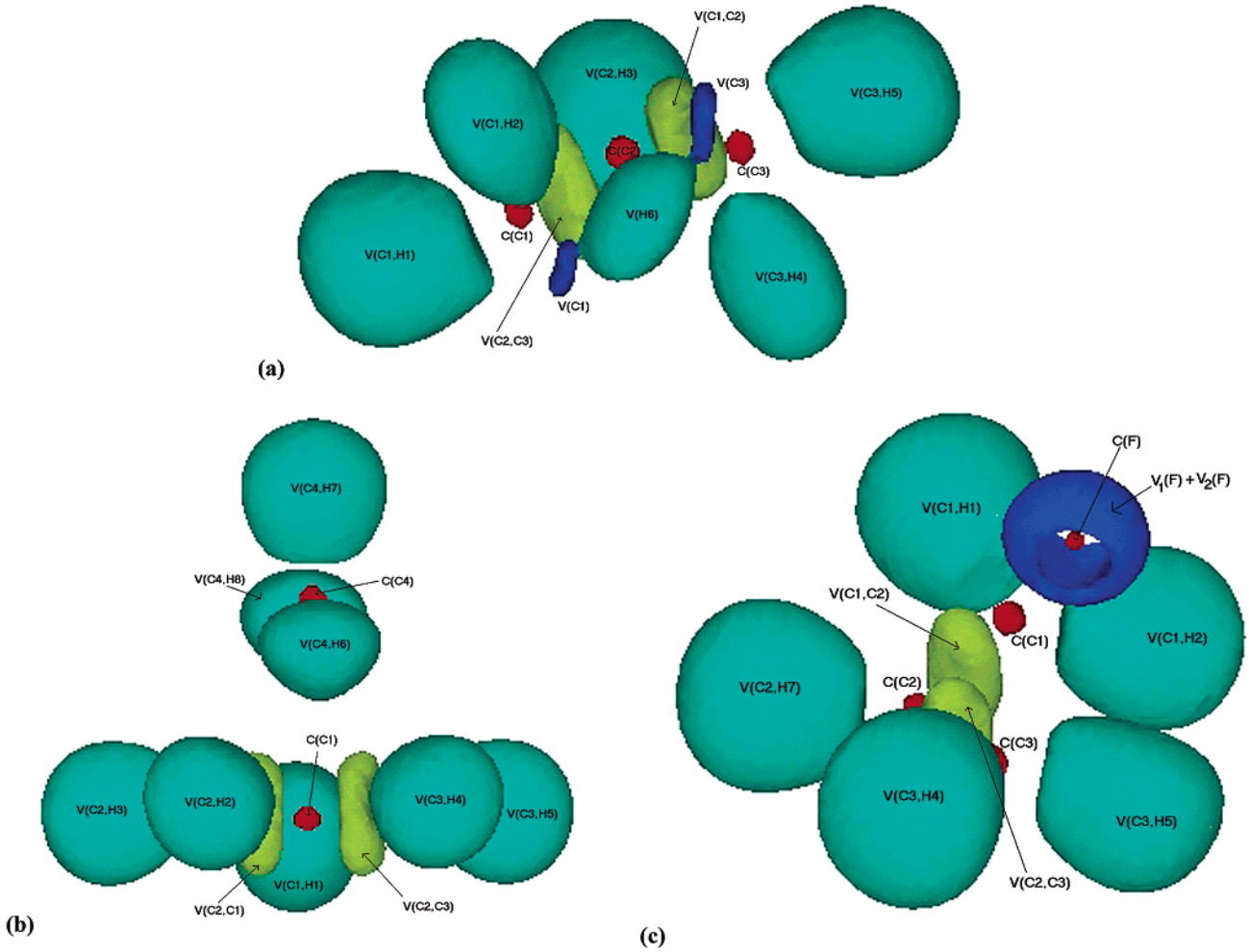


**Figure 2.** Localization domains of the ELF at the transition state of the (a) [$1_s$,$3_a$]hydrogen, (b) [$1_a$,$3_s$]methyl, and (c) [$1_a$,$3_s$]fluorine sigmatropic shift reactions in the allyl system. The ELF = 0.80 isosurfaces were calculated from the optimized wave functions at the B3LYP/6-311++G(d,p) level of theory.

B3LYP/6-311++G(d,p) level of theory. Stationary points have been fully characterized using the vibrational analysis. The symmetry allowed [$1_s$,$3_a$]hydrogen, [$1_a$,$3_s$]methyl, and [$1_a$,$3_s$]-fluorine TSs to be found with a unique imaginary frequency, and the intrinsic reaction coordinate (IRC) pathway[66] connecting each with the corresponding reactant and product conformations was calculated. The evaluation of the topological analysis of ELF function defined in eq 1 and its gradient field-associated properties, eqs 2−7, has been obtained and analyzed using the TopMod[67,68] and the visualization Vis5d[69] series of programs.

## Results and Discussion

Figure 1 schematizes the geometrical structure for each optimized TS. The topology of the electron localization domains (represented by the ELF = 0.80 isosurface) for the three symmetry-allowed TSs is depicted in Figure 2. The corresponding bifurcation diagrams are depicted in Figure 3. The topological ELF results based on the B3LYP/6-311++G(d,p)-optimized density are presented in Tables 1−3 for the [$1_s$,$3_a$]hydrogen, the [$1_a$,$3_s$]methyl, and the [$1_a$,$3_s$]fluorine sigmatropic migrations, respectively. These tables show the calculated basin populations $\tilde{N}_i$, variances $\sigma^2(\tilde{N}_i)$, relative fluctuations $\lambda(\tilde{N}_i)$, and main contributions from other basins $i$ (%) to $\sigma^2(\tilde{N}_i)$ for each TS. Although core basin populations and related properties do not have a relevant role for the description of the observed reactivity patterns along the sigmatropic rearrangements, this information has been included for completeness of the present analysis.

**Hydrogen Migration.** The [$1_s$,$3_a$]hydrogen sigmatropic shift is a degenerate rearrangement, which has been previously characterized at several levels of theory. The earliest results were based on RHF/STO-3G-[15] and RHF/4-31G-optimized[16] stationary points. Single point calculations on the RHF/4-31G structure including 3 × 3CI, RHF/DZ, RHF/DZP, IEPA/DZ, IEPA/DZP, PNO-CI/DEZP, and CEPA/DZP levels were also presented.[16] MC-SCF calculations suggested that the forbidden [$1_s$,$3_s$] pathway does not exist for the 1,3 shift in propene.[18] Results from complete optimizations at the RHF/3-21G, RHF/6-31G, RHF/6-31G(d), and MP2/6-31G(d)//RHF/6-31G levels of theory have also been reported, including the existence of a higher energy TS with a $C_{2v}$ symmetry.[19] Structural data for the TS at the CASSCF/6-31G(d) level are also known.[24] All of these results have been interpreted in light of the Woodward−Hoffmann orbital symmetry principles, and a favored antarafacial pathway is now firmly established.[5] Our present analysis focuses directly for the first time on the bonding nature of the TS based on the ELF, a local measure of the Pauli repulsion effects.

The irreducible representation domains bounded by the ELF = 0.80 isosurface at the transition state of the [$1_s$,$3_a$]hydrogen, [$1_a$,$3_s$]methyl, and [$1_a$,$3_s$]fluorine sigmatropic shift reactions in the allyl system are schematized in Figure 2a−c, respectively. In red are represented the three core basins, C(C1), C(C2), and C(C3), corresponding to the carbon atoms; in green are represented the five V(C,H) protonated disynaptic basins,

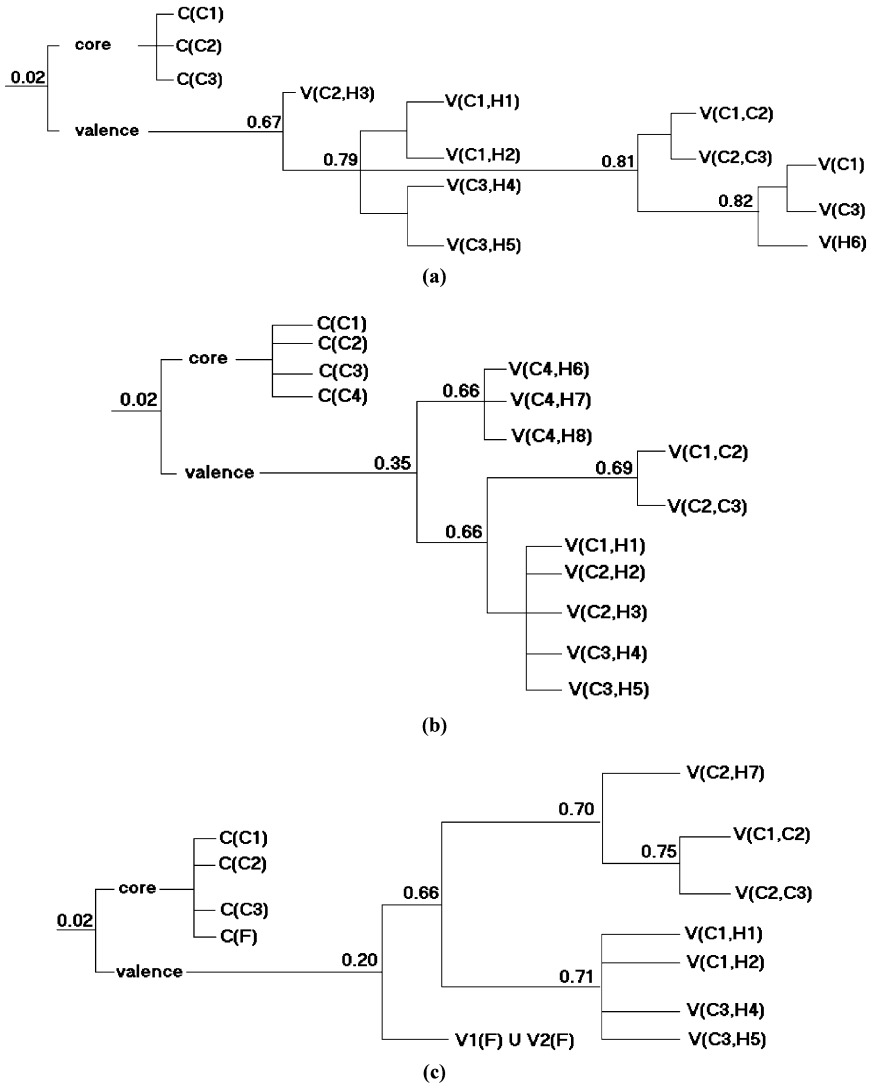


**Figure 3.** Bifurcation diagrams corresponding to the ELF analysis at the transition state of the (a) [$1_s$,$3_a$]hydrogen, (b) [$1_a$,$3_s$]methyl, and (c) [$1_a$,$3_s$]fluorine sigmatropic shift reactions in the allyl system, from the optimized wave functions at the B3LYP/6-311++G(d,p) level of theory.

corresponding to the single bond between the C and the H atoms; and in brilliant green are represented two disynaptic valence basins, V(C1,C2) and V(C2,C3), which correspond to the rearranging pairs of CC bonds. There are also three valence attractors associated directly with the migration of the hydrogen atom and the rearrangement of the two V(C,C) densities: two valence monosynaptic basins are associated with the terminal carbons, V(C1) and V(C3), schematized in blue, and one valence monosynaptic basin V(H6), depicted in green, appears directly at the position of the migrating hydrogen atom. The valence V(C1) and V(C3) basins are localized above and below the molecular plane, and their volume shapes are highly distorted. The position and shape of the located valence basins V(C1,C2), V(C2,C3), V(C1), V(C3), and V(H6) can be related explicitly with the intuitive view of the distortion of the electron flow along the rearrangement as expected for an antarafacial [$1_s$,$3_a$]hydrogen sigmatropic shift. It is clear that a more detailed analysis of the electron rearrangement along the pericyclic pathway can be taken by resorting to the analysis of the electronic populations and its associated relative quantum fluctuations.

In Table 1, the electron properties derived from integration of the electron density in the ELF basins are reported. It can be immediately noted that there are four types of different basins, which differ on the quantum uncertainty ($\sigma^2$) or in the relative fluctuation ($\lambda$) values. Carbon atom core populations, C(C), are centered on 2.1e with the lowest delocalization values ($\lambda = 0.1$); the C−H bond valence populations of 1.9e and 2.1e appear with intermediate delocalization values ($\lambda = 0.3-0.4$); the C−C bond valence populations of 2.5e appear with slightly higher values of delocalization ($\lambda = 0.5$); and finally, the populations associated with the migration of the hydrogen atom V(H6) (1.0e) and the rearrangement of the two CC bonds densities (2.5e) appear with the highest values of delocalization ($\lambda = 0.7-0.8$). From the contribution analysis data, we will note below that there is a noticeable electronic delocalization involving some set of basins. The populations are being delocalized mainly between the neighborhood basins; the shape and extent of this exchange, as we will see below, are unique characteristics for each stationary point. It must be noted that for the core populations, the exchange occurs only through the bond line connecting the basins but for the C−H and the C−C valence population basins this indeed occurs through spatial interactions. Core fluctuations are not very important because of their high localization population values. More interesting is the valence analysis, which reveals explicitly the form of a delocalized bonding of the complete [$1_s$,$3_a$] TS structure. We can see, for instance, that the V(C2,H3) basin population is noticeably delocalized with the V(C1,C2) and V(C2,C3) basins (32.4%), and the V(C1,H1) population is delocalized on V(C1,H2)

**TABLE 1: ELF Basin Populations $\tilde{N}i$, Variance $\sigma^2(\tilde{N}i)$, Relative Fluctuation $\lambda(\tilde{N}i)$, and Main Contributions of Other Basins *i* (%) to $\sigma^2(\tilde{N}i)$, Corresponding to TS $[1_s,3_a]$H at the B3LYP/6-311++G(d,p) Level of Theory**

| | basin | $\tilde{N}i$ | $\sigma^2(\tilde{N}i)$ | $\lambda(\tilde{N}i)$ | contribution analysis (%) |
|---|---|---|---|---|---|
| **1** | C(C1) | 2.1 | 0.3 | 0.1 | **4**(28.0), **5**(22.8), **10**(11.4), **11**(27.8) |
| **2** | C(C2) | 2.1 | 0.3 | 0.1 | **6**(29.0), **11**(29.2), **12**(29.2) |
| **3** | C(C3) | 2.1 | 0.3 | 0.1 | **7**(22.8), **8**(28.0), **12**(27.8), **13**(11.4) |
| **4** | V(C1,H1) | 2.1 | 0.7 | 0.3 | **1**(10.8), **5**(28.7), **9**(5.2), **10**(16.7), **11**(27.4) |
| **5** | V(C1,H2) | 1.9 | 0.7 | 0.4 | **1**(8.1), **4**(26.4), **9**(12.1), **10**(14.7), **11**(25.7) |
| **6** | V(C2,H3) | 2.7 | 0.6 | 0.3 | **2**(11.7), **11**(32.4), **12**(32.4) |
| **7** | V(C3,H4) | 1.9 | 0.7 | 0.4 | **3**(8.1), **8**(26.4), **9**(12.1), **12**(25.7), **13**(14.7) |
| **8** | V(C3,H5) | 2.1 | 0.7 | 0.3 | **3**(10.8), **7**(28.7), **9**(5.3), **12**(27.4), **13**(16.8) |
| **9** | V(H6) | 1.0 | 0.6 | 0.7 | **4**(5.6), **5**(14.1), **7**(14.1), **8**(5.6), **10**(18.3), **11**(8.8), **12**(8.8), **13**(18.3) |
| **10** | V(C1) | 0.8 | 0.6 | 0.8 | **1**(4.9), **4**(18.6), **5**(17.9), **6**(4.1), **7**(3.4), **9**(19.9), **11**(24.6), **12**(4.8) |
| **11** | V(C1,C2) | 2.5 | 1.2 | 0.5 | **1**(5.9), **2**(6.1), **4**(15.5), **6**(16.9), **9**(4.6), **10**(12.2), **12**(17.2) |
| **12** | V(C2,C3) | 2.5 | 1.2 | 0.5 | **2**(6.2), **3**(5.9), **6**(16.9), **7**(15.4), **8**(15.1), **9**(4.5), **11**(17.1), **13**(12.3) |
| **13** | V(C3) | 0.8 | 0.6 | 0.7 | **3**(4.9), **5**(3.4), **6**(4.1), **7**(17.9), **8**(18.6), **9**(19.9), **11**(4.8), **12**(24.6) |

**TABLE 2: ELF Basin Populations $\tilde{N}i$, Variance $\sigma^2(\tilde{N}i)$, Relative Fluctuation $\lambda(\tilde{N}i)$, and Main Contributions of Other Basins *i* (%) to $\sigma^2(\tilde{N}i)$, Corresponding to TS $[1_a,3_s]CH_3$ at the B3LYP/6-311++G(d,p) Level of Theory**

| | basin | $\tilde{N}i$ | $\sigma^2(\tilde{N}i)$ | $\lambda(\tilde{N}i)$ | contribution analysis (%) |
|---|---|---|---|---|---|
| **1** | C(C1) | 2.1 | 0.3 | 0.1 | **5**(27.0), **13**(32.5), **14**(32.5) |
| **2** | C(C2) | 2.1 | 0.3 | 0.1 | **6**(28.0), **7**(29.0), **14**(33.8) |
| **3** | C(C3) | 2.1 | 0.3 | 0.1 | **8**(28.0), **9**(29.0), **13**(33.8) |
| **4** | C(C4) | 2.1 | 0.3 | 0.1 | **10**(31.3), **11**(29.1), **12**(32.2) |
| **5** | V(C1,H1) | 2.1 | 0.7 | 0.3 | **1**(10.8), **6**(3.7), **7**(4.3), **8**(3.7), **9**(4.3), **13**(34.2), **14**(34.2) |
| **6** | V(C2,H2) | 2.2 | 0.7 | 0.3 | **2**(10.7), **5**(3.6), **7**(30.0), **10**(6.9), **12**(3.6), **13**(3.6), **14**(36.9) |
| **7** | V(C2,H3) | 2.2 | 0.7 | 0.3 | **2**(11.2), **5**(4.2), **6**(30.4), **10**(4.6), **12**(3.7), **13**(3.3), **14**(38.4) |
| **8** | V(C3,H4) | 2.2 | 0.7 | 0.3 | **3**(10.7), **5**(3.6), **9**(30.0), **10**(6.9), **12**(3.6), **13**(36.9), **14**(3.6) |
| **9** | V(C3,H5) | 2.2 | 0.7 | 0.3 | **3**(11.2), **5**(4.2), **8**(30.4), **10**(4.6), **12**(3.7), **13**(38.4), **14**(3.3) |
| **10** | V(C4,H6) | 2.4 | 0.9 | 0.4 | **4**(9.2), **6**(3.0), **7**(3.2), **8**(3.0), **9**(3.2), **11**(32.5), **12**(30.0), **13**(6.8), **14**(6.9) |
| **11** | V(C4,H7) | 2.2 | 0.7 | 0.3 | **4**(11.3), **10**(36.1), **12**(36.1), **13**(3.9), **14**(3.9) |
| **12** | V(C4,H8) | 2.4 | 0.8 | 0.3 | **4**(9.2), **6**(3.0), **7**(3.2), **8**(3.0), **9**(3.2), **10**(32.5), **11**(30.0), **13**(6.8), **14**(6.9) |
| **13** | V(C1,C3) | 2.9 | 1.4 | 0.5 | **1**(6.1), **3**(6.4), **5**(16.6), **8**(18.1), **9**(18.7), **10**(4.1), **12**(4.0), **14**(20.3) |
| **14** | V(C1,C2) | 2.9 | 1.4 | 0.5 | **1**(6.1), **2**(6.4), **5**(16.6), **6**(18.1), **7**(18.7), **10**(4.1), **12**(4.0), **13**(20.3) |

(28.7%), V(C1,C2) (27.4%), and V(C1) (16.7%) basins. The V(C1,H2) population is being delocalized with V(C1,C2) (27.4%), V(C1) (16.7%), and V(H6) (12.1%) basins. The behavior of V(C3,H4) and V(C3,H5) is found symmetric to those of V(C1,H2) and V(C1,H1) basin populations, respectively. Fluctuation patterns corresponding to the V(C,C) emphasize the great coupling of bonding. It can be noted that main contributions arise from the neighbors, V(C,C) and V(C,H) basins, as well as the closest V(C) basin. For instance, the pattern of contribution analysis for V(C3,C2) is 17.2% with the V(C1,C2) basin, 15.4% with the V(C3,H4) basin, and 12.3% with the V(C3) basin. The migrating hydrogen atom population at V(H6) shows contributions of 18.4% with both V(C1) and V(C3) basins, 14.1% with the closest V(C,H) basins (i.e., H2 and H4), and 8.8% with each V(C,C) basins. The V(C1) population depicts a pattern of fluctuation involving mainly the V(C1,C2) (24.6%) basin and the V(H6) basin (19.9%) with important contributions arising from the V(C1,H1) and V(C1,H2) (18.6%) basins. The V(C3) basin population shows the corresponding symmetry-related pattern to V(C1).

It is thus evident from the topological analysis of the ELF for the antarafacial TS that it can be visualized effectively as a strongly dynamical delocalized entity, which agrees with a pericyclic process in a sense that extends and complements (in semiquantitatively) the view based only on orbital symmetry considerations. In this context and from the contribution analysis data, the key role of the valence V(C−H) basins is emphasized as a dynamical and transitory natural reservoirs for the rearrangement of the fluxing electron density. It must also be noted that global symmetry constraints are conserved and reflected in the ELF analysis of the corresponding TS.

**Methyl Migration.** As it is known, the Woodward−Hoffmann-allowed $[1_a,3_s]$alkyl migration process involves a suprafacial stereochemistry with inversion at the migrating center.[2−5,25] Figure 2b depicts the calculated ELF domains of localization for the corresponding TS. There are represented four monosynaptic core basins C(Ci), in red, corresponding to each carbon atom, eight disynaptic valence protonated V(C,H) basins, in green, corresponding to the C−H bond regions, and two disynaptic valence V(C,C) basins, in brilliant green, corresponding to the two CC bonds. It can also be noted that there is not any polisynaptic basin connecting the methyl and the allyl fragments. Furthermore, it will be seen from the fluctuation analysis that populations on these fragments are not exchanged between them. Thus, it can be observed from Table 2 that the valence-protonated basin populations are centered on 2.1e−2.4e and it has intermediate delocalization values ($\lambda = 0.3-0.4$). The fluctuation analysis indicates that as expected, electron density is delocalized mainly on the closest valence and core basins. The observed fluctuation patterns for both the allyl and the methyl fragments indicate that they are effectively separated species at the TS. For instance, we can see that V(C4,H6), V(C4,H7), and V(C4,H8) are delocalized on the C(C4) (9.2, 11.3, and 10.3%, respectively) and noticeably between themselves (>30% each). This view is reinforced by the fact that the two V(C,C) valence basins have major fluctuations only with basins on the allyl fragment. For instance, the population of the V(C1,C3) basin is exchanged 20.3% with those from the V(C2,C3) basin, 18.0% with both the V(C3,H9) and the V(C3,H8) basins and 16.4% with the V(C1,H5) basin. Indeed, the total number of electrons at the methyl and allyl fragments (9.1e and 23.1e, respectively) reveals, after introducing nuclear charges, that the TS can be rationalized directly as two weakly interacting methyl and allyl radicals. It is interesting to note again that all of these analyses have been done without resorting to either orbitals or symmetry requirement arguments. We need to emphasize at this point that the topology from the ELF analysis has been shown to be independent enough of the level of theory being used.

**Fluorine Migration.** The topological analysis of the ELF for the $[1_a,3_s]$fluorine migration in the allyl system has been

**TABLE 3: ELF Basin Populations $\tilde{N}i$, Variance $\sigma^2(\tilde{N}i)$, Relative Fluctuation $\lambda(\tilde{N}i)$, and Main Contributions of Other Basins $i$ (%) to $\sigma^2(\tilde{N}i)$, Corresponding to TS [$1_a$,$3_s$]F at the B3LYP/6-311++G(d,p) Level of Theory**

| | basin | $\tilde{N}i$ | $\sigma^2(\tilde{N}i)$ | $\lambda(\tilde{N}i)$ | contribution analysis (%) |
|---|---|---|---|---|---|
| **1** | C(C1) | 2.1 | 0.3 | 0.1 | **5**(29.3), **6**(30.1), **10**(31.5), **11**(3.3) |
| **2** | C(C2) | 2.1 | 0.3 | 0.1 | **7**(28.3), **10**(30.5), **11**(31.5) |
| **3** | C(C3) | 2.1 | 0.3 | 0.1 | **8**(29.3), **9**(30.1), **11**(31.5), **10**(3.3) |
| **4** | C(F) | 2.1 | 0.4 | 0.2 | **12**(64.9), **13**(30.8) |
| **5** | V(C1,H1) | 2.1 | 0.6 | 0.3 | **1**(12.0), **6**(32.2), **7**(4.6), **10**(34.4), **11**(5.8), **12**(4.8), **13**(3.4) |
| **6** | V(C1,H2) | 2.1 | 0.7 | 0.3 | **1**(11.7), **5**(30.5), **7**(3.6), **10**(32.0), **11**(5.2), **12**(9.0), **13**(3.9) |
| **7** | V(C2,H3) | 2.1 | 0.7 | 0.3 | **2**(11.2), **5**(4.3), **6**(3.5), **8**(4.3), **9**(3.5), **10**(34.3), **11**(35.0) |
| **8** | V(C3,H4) | 2.1 | 0.6 | 0.3 | **3**(12.0), **7**(4.6), **9**(32.2), **10**(5.8), **11**(34.8), **12**(4.8), **13**(3.4) |
| **9** | V(C3,H5) | 2.1 | 0.7 | 0.3 | **3**(11.7), **7**(3.6), **8**(30.5), **10**(5.2), **11**(32.0), **12**(9.0), **13**(3.9) |
| **10** | V(C1,C2) | 2.7 | 1.3 | 0.5 | **1**(6.4), **2**(6.2), **5**(16.8), **6**(16.2), **7**(18.0), **11**(24.1), **12**(3.5) |
| **11** | V(C2,C3) | 2.7 | 1.3 | 0.5 | **2**(6.4), **3**(6.2), **7**(18.0), **8**(16.8), **9**(16.2), **10**(24.1), **12**(3.5) |
| **12** | $V_1$(F) | 5.1 | 1.5 | 0.3 | **4**(17.1), **6**(4.1), **9**(4.1), **10**(3.1), **11**(3.2), **13**(63.2) |
| **13** | $V_2$(F) | 2.4 | 1.2 | 0.5 | **4**(9.7), **10**(2.9), **11**(3.0), **12**(75.8) |

recently explored at the B3PW91/6-311G(d,p) level of theory.[62] The Woodward−Hoffmann-allowed Cs suprafacial TS was rationalized as a fluorine−allyl ion−pair with a charge separation of 0.6e. From Figure 2c and Table 3, we can see that at the present level of calculation all of the topological characteristics are retained. In the present representation, we have four core attractors, in red, corresponding to the three carbon atoms, C(C), and to the F atom, C(F). There are also five V(C,H) basins, in green, corresponding to the C−H bonds, while the valence region of the halogen atom is divided by two attractors, $V_1$(F) and $V_2$(F), in blue, with a basin population of 7.5e. The five V(C,H) basins again show intermediate delocalization values ($\lambda = 0.3$) for populations centered on 2.1e, while the V(C,C) and V(F) basins are the most delocalized populations ($\lambda = 0.5$). There is not any polisynaptic basin connecting the fluorine and allyl fragments. From the basin-integrated density calculations, electron populations in both spatial basin regions yield a charge separation in the sense of $F^{(-0.6e)} \ldots C_3H_5^{(+0.6e)}$. The observed fluctuation patterns for C(F) and $V_i$(F) on the halogen center, and for the valence populations on the allyl part, agree with the view of an ion−pair interaction with some delocalization among the allyl spatial regions.[62] Note again that these conclusions have been drawn only on the basis of the topology of the ELF function, a measure of the local excess of kinetic energy due to the Pauli principle.

**Bifurcation Diagrams.** With the aim to help in the present discussion and clarify the differences between the three mechanisms and the new insights provided by the ELF partition technique, we have also obtained the bifurcation diagrams corresponding to the [$1_s$,$3_a$]hydrogen, [$1_a$,$3_s$]methyl, and [$1_a$,$3_s$]-fluorine sigmatropic shift reactions. These are schematized in Figure 3a−c, respectively. It can be noted that for the antarafacial hydrogen migration, the bifurcation diagram shows a unique reducible valence domain for the V(C1), V(C3), and V(H6), which is separated at ELF = 0.82. In the case of methyl and fluorine [1,3] migrations, the valence−valence separation between the allylic moiety and either the $CH_3$ or the $F^-$ takes place effectively at lower ELF values, 0.35 and 0.20, respectively. Bifurcation diagrams complement the population analysis reported in Tables 1−3, emphasizing and characterizing uniquely the nature of bonding in the [$1_s$,$3_a$]hydrogen, the [$1_a$,$3_s$]methyl, and the [$1_a$,$3_s$]fluorine sigmatropic rearrangements in terms of a highly delocalized one, a two radicals interaction one, and an ion−pair interaction one, respectively.

## Concluding Remarks

It has been shown that the topological analysis of the ELF is capable of describing the bonding nature of the allowed [$1_s$,$3_a$]-hydrogen, [$1_a$,$3_s$]methyl, and [$1_a$,$3_s$]fluorine TSs corresponding to the sigmatropic shift in the allyl system. A semiquantitative description, which agrees well with the traditional intuitive picture of bonding, is reached for each stationary point. For this type of one step unimolecular process, the TS resembles a highly delocalized one in the case of hydrogen transfer, a two radical interaction in the case of methyl migration, and an ion−pair separation in the case of fluorine rearrangement. The basin properties calculated from the B3LYP/6-311++G(d,p) density allow us to draw conclusions, which agree and complement the standard Woodward−Hoffmann symmetry orbital-based analysis. This fact is a remarkable result because the single analysis of bonding using the ELF tool is based formally only on the local kinetic energy excess due to the Pauli repulsion, without using any of the frontier molecular orbital interactions.

**Acknowledgment.** We thank Prof. Andreas Savin for an illuminating discussion about the ELF. This work has been supported by FONDECYT (Fondo de Desarrollo Científico y Tecnológico, Chile) under Grants No. 2990030, No. 2000085, No. 2000092, No. 1000816, and No. 1010649. E.C., B.G., and J.C.S. thank the DAAD (Deutscher Akademischer Austauschdienst, Germany) for Ph.D. fellowships. E.C. and J.C.S. thank the Universidad de Chile-Mecesup Grant UCH0008. We thank the referees for the critical review and useful comments regarding this work.

## References and Notes

(1) Wiest, O.; Montiel, D. C.; Houk, K. N. *J. Phys. Chem. A* **1997**, *101*, 8378.
(2) Woodward, R. B.; Hoffmann, R. *J. Am. Chem. Soc*. **1965**, *87*, 395.
(3) Hoffmann, R.; Woodward, R. B. *J. Am. Chem. Soc*. **1965**, *87*, 2046, 4389.
(4) Woodward, R. B.; Hoffmann, R. *Angew. Chem. Int., Ed. Engl*. **1969**, *8*, 781.
(5) Woodward, R. B.; Hoffmann, R. *The Conservation of Orbital Symmetry*; Academic Press: New York, 1970.
(6) Kato, S. *Theor. Chem. Acc.* **2000**, *103*, 219.
(7) Fukui, K. *Acc. Chem. Res.* **1971**, *4*, 57.
(8) Dewar, M. J. S. *Angew. Chem., Int. Ed. Engl*. **1971**, *10*, 761.
(9) Zimmerman, H. E. *Acc. Chem. Res*. **1971**, *4*, 272.
(10) Pasto, D. J.; Brophy, J. E. *J. Am. Chem. Soc*. **1991**, *56*, 4554.
(11) Yeh, M.-H.; Linder, L.; Hoffmann, D. K.; Barton, T. J. *J. Am. Chem. Soc*. **1986**, *108*, 7849.
(12) So, S. P. *Chem. Phys. Lett.* **1996**, *254*, 302.
(13) Jensen, F. *J. Am. Chem. Soc.* **1995**, *117*, 7487.
(14) Nguyen, M.; Landuyt, L.; Vanquickenborne, L. G. *Chem. Phys. Lett*. **1993**, *212*, 543.
(15) Bouma, W. J.; Vicent, M. A.; Radom, L. *Int. J. Quantum Chem*. **1978**, *14*, 767.
(16) Rodwell, W. R.; Bouma, W. J.; Radom, L. *Int. J. Quantum Chem.* **1980**, *18*, 107.
(17) Hess, B. A.; Schaad, L. J. *J. Am. Chem. Soc.* **1983**, *105*, 7185.
(18) Bernardi, F.; Robb, M. A.; Schlegel, H. B.; Tonachini, G. *J. Am. Chem. Soc.* **1984**, *106*, 1198.
(19) Hess, B. A.; Schaad, L. J.; Pancir, J. *J. Am. Chem. Soc*. **1985**, *107*, 149.
(20) Dormans, G. J. M.; Buck, H. M. *J. Am. Chem. Soc*. **1986**, *108*, 3253.
(21) Dormans, G. J. M.; Buck, H. M. *THEOCHEM* **1986**, *136*, 121.
(22) Poirier, R. A.; Majlessi, D.; Zielinski, T. J. *J. Comput. Chem*. **1986**, *7*, 464.
(23) Scroder, S.; Thiel, W. *J. Am. Chem. Soc.* **1986**, *108*, 7985.

(24) Houck, K. N.; Li, Y.; Evanseck, J. D. *Angew. Chem., Int. Ed. Engl.* **1992**, *31*, 682.
(25) Berson, J. A. *Acc. Chem. Res.* **1972**, *5*, 406.
(26) See, for instance: (a) Berson, J. A. *Acc. Chem. Res.* **1972**, *5*, 406. (b) Berson, J. A.; Holder, R. W. *J. Am. Chem. Soc.* **1973**, *95*, 2037.
(27) Becke, A. D.; Edgencombe, K. E. *J. Chem. Phys.* **1990**, *92*, 5397.
(28) Savin, A.; Nesper, R.; Wengert, S.; Fäsler, T. F. *Angew. Chem., Int. Ed. Engl.* **1997**, *36*, 1808.
(29) Marx, D.; Savin, A. *Angew. Chem., Int. Ed. Engl.* **1997**, *36*, 2077.
(30) Grin, Y.; Wedig, U.; Wagner, F.; von Schnering, H. G.; Savin, A. *J. Alloys Compd.* **1997**, *255*, 203.
(31) Kohout, M.; Savin, A. *J. Comput. Chem.* **1997**, *18*, 1431.
(32) Kohout, M.; Savin, A. *Int. J. Quantum Chem.* **1996**, *60*, 875.
(33) Savin, A.; Silvi, B.; Colonna, F. *Can J. Chem.* **1996**, *74*, 1088.
(34) Silvi, B.; Savin, A. *Nature (London)* **1994**, *371*, 683.
(35) Noury, S.; Colonna, F.; Savin, A.; Silvi, B. *J. Mol. Struct.* **1998**, *59*, 450.
(36) Alikhani, M. E.; Bouteiller, Y.; Silvi, B. *J. Phys. Chem.* **1996**, *100*, 16092.
(37) Fourré, I.; Silvi, B.; Chaquin, P.; Savin, A. *J. Comput. Chem.* **1999**, *20*, 897.
(38) Llusar, R.; Beltrán, A.; Andrés, J.; Noury, S.; Silvi, B. *J. Comput. Chem.* **1999**, *20*, 1517.
(39) Beltrán, A.; Andrés, J.; Noury, S.; Silvi, B. *J. Phys. Chem. A* **1999**, *103*, 3078.
(40) Berski, S.; Silvi, B.; Latajka, Z.; Leszczynski, J. *J. Chem. Phys.* **1999**, *111*, 2542.
(41) Fuster, F.; Sevin, A.; Silvi, B. *J. Phys. Chem. A* **2000**, *104*, 852.
(42) Fuentealba, P.; Savin, A. *J. Phys. Chem. A* **2001**, *105*, 11531.
(43) Krokidis, X.; Noury, S.; Silvi, B. *J. Phys. Chem. A* **1997**, *101*, 7277.
(44) Krokidis, X.; Goncalves, V.; Savin, A.; Silvi, B. *J. Phys. Chem. A* **1998**, *102*, 5065.
(45) Krokidis, X.; Silvi, B.; Alikhani, M. E. *Chem. Phys. Lett.* **1998**, *292*, 35.
(46) Chamorro, E.; Toro-Labbé, A.; Fuentealba, P. *J. Phys. Chem. A* **2002**, *106*, 3891.
(47) Krokidis, X.; Vuilleumier, R.; Borgir, D.; Silvi, B. *Mol. Phys.* **1999**, *96*, 265.
(48) Wang, Y. X.; Flad, H. J.; Dolg, M. *J. Phys. Chem. A* **2000**, *104*, 5558.
(49) Chevreau, H.; Sevin, A. *Chem. Phys. Lett.* **2000**, *322*, 9.
(50) Choukroun, R.; Donnadieu, B.; Zhao, J. S.; Cassoux, P.; Lepetit, C.; Silvi, B. *Organometallics* **2000**, *19*, 1901.
(51) Fuster, F.; Sevin, A.; Silvi, B. *J. Comput. Chem.* **2000**, *21*, 509.
(52) De Santis, L.; Resta, R. *Surf. Sci.* **2000**, *450*, 126.
(53) Silvi, B.; Gatti, C. *J. Phys. Chem. A* **2000**, *104*, 947.
(54) Chestnut, D. B.; Bartolotti, J. *Chem. Phys.* **2000**, *253*, 1.
(55) Fuster, F.; Silvi, B. *Chem. Phys.* **2000**, *252*, 279.
(56) Fassler, T. J.; Hoffmann, S. *Z. Anorg. Allg. Chem.* **2000**, *626*, 1, 106.
(57) Frison, G.; Sevin, A. *J. Phys. Chem. A* **1999**, *103*, 10998.
(58) Krokidis, X.; Moriarty, N. M.; Lester, W. A.; Frenklach, M. *Chem. Phys. Lett.* **1999**, *314*, 534.
(59) Chattaraj, P. K.; Chamorro, E.; Fuentealba, P. *Chem. Phys. Lett.* **1999**, *314*, 114.
(60) Fuentealba, P.; Savin, A. *J. Phys. Chem. A* **2000**, *104*, 10882.
(61) See, for example: (a) Fassler, T.; Hoffmann, S.; Kronseder, C. *Z. Anorg. Allg. Chem.* **2001**, *627*, 2486. (b) Chesnut, D. B. *J. Comput. Chem.* **2001**, *22*, 1702. (c) Moc, J.; Panek, J. *Chem. Phys. Lett.* **2001**, *345*, 497. (d) Llusar, R.; Beltran, A.; Andres, J.; Fuster, F.; Silvi, B. *J. Phys. Chem. A* **2001**, *105*, 9460. (e) Zurcher, F.; Nesper, R.; Hoffmann, S.; Fassler, T. F. *Z. Anorg. Allg. Chem.* **2001**, *627*, 2211. (f) Chesnut, D. B. *Chem. Phys.* **2001**, *271*, 9. (g) Fressigne, C.; Maddaluno, J.; Giessner-Prettre, C.; Silvi, B. *J. Org. Chem.* **2001**, *66*, 6476. (h) Platts, J. A. *THEOCHEM* **2001**, *545*, 111. (i) Berski, S.; Jaszewski, A. R.; Jezierska, J. *Chem. Phys. Lett.* **2001**, *341*, 168. (j) Oliva, M.; Safont, V. S.; Andres, J.; Tapia, O. *Chem. Phys. Lett.* **2001**, *340*, 391. (k) Molina, J.; Dobado, J. A. *Theor. Chem. Acc.* **2001**, *105*, 328. (l) Sun, Q.; Wang, Q.; Yu, J. Z.; Kumar, V.; Kawazoe, Y. *Phys. Rev. B: Condens. Matter Mater. Phys.* **2001**, *63*, 193408/1. (m) Isea, R. *THEOCHEM* **2001**, *540*, 131. (n) Chevreau, H.; de Moreira, I.; Silvi, B.; Illas, F. *J. Phys. Chem. A* **2001**, *105*, 3570. (o) Berski, S.; Latajka, Z.; Silvi, B.; Lundell, J. *J. Chem. Phys.* **2001**, *114*, 4349. (p) Tampier, M.; Johrendt, D. *Z. Anorg. Allg. Chem.* **2001**, *627*, 312. (q) Panek, J.; Latajka, Z. *Chem. Phys. Lett.* **2000**, *332*, 617.
(62) Chamorro, E.; Santos, J. C.; Gómez, B.; Contreras, R.; Fuentealba, P. *J. Chem. Phys.* **2001**, *114*, 23.
(63) Savin, A.; Becke, A. D.; Flad, J.; Nesper, R.; Preuss, H.; von Schnering, H. *Angew. Chem., Int. Ed. Engl.* **1991**, *30*, 409.
(64) Bader, R. F. W. *Localization and Delocalization in Quantum Chemistry*; Chalvet, O., et al., Eds.; Reidel: Dordrecht, 1976; Vol. 1.
(65) Frisch, M. J.; Trucks, G. W.; Schlegel, H. B.; Scuseria, G. E.; Robb, M. A.; Cheeseman, J. R.; Zakrzewski, V. G.; Montgomery, J. A., Jr.; Stratmann, R. E.; Burant, J. C.; Dapprich, S.; Millam, J. M.; Daniels, A. D.; Kudin, K. N.; Strain, M. C.; Farkas, O.; Tomasi, J.; Barone, V.; Cossi, M.; Cammi, R.; Mennucci, B.; Pomelli, C.; Adamo, C.; Clifford, S.; Ochterski, J.; Petersson, G. A.; Ayala, P. Y.; Cui, Q.; Morokuma, K.; Malick, D. K.; Rabuck, A. D.; Raghavachari, K.; Foresman, J. B.; Cioslowski, J.; Ortiz, J. V.; Baboul, A. G.; Stefanov, B. B.; Liu, G.; Liashenko, A.; Piskorz, P.; Komaromi, I.; Gomperts, R.; Martin, R. L.; Fox, D. J.; Keith, T.; Al-Laham, M. A.; Peng, C. Y.; Nanayakkara, A.; Challacombe, M.; Gill, P. M. W.; Johnson, B.; Chen, W.; Wong, M. W.; Andres, J. L.; Gonzalez, C.; Head-Gordon, M.; Replogle, E. S.; Pople, J. A. *Gaussian 98*, Revision A.9; Gaussian, Inc.: Pittsburgh, PA, 1998.
(66) Gonzalez, C.; Schlegel, H. B. *J. Phys. Chem.* **1990**, *94*, 5523.
(67) Noury, S.; Krokidis, X.; Fuster, F.; Silvi, B. *TopMoD Package*; Universite Pierre et Marie Curie, 1997.
(68) Noury, S.; Krokidis, X.; Fuster, F.; Silvi, B. *Comput. Chem.* **1999**, *23*, 597.
(69) (a) Hibbard, B.; Kellum, J.; Paul, B. *Vis5d 5.1, Visualization Project*; University of Winconsin-Madison Space Science and Engineering Center (SSEC). (b) Hibbard, B.; Santek, D. *Proc. IEEE Visualization '90*, **1990**, 129.